When NMDA Receptor Conductances increase Inter-Spike Interval Variability

Giancarlo La Camera, Stefano Fusi, Walter Senn, Alexander Rauch and Hans-R. Lüscher

Institute of Physiology, University of Bern, Bühlplatz 5, 3012 Bern, Switzerland
{lacamera,fusi,senn,rauch,luescher}@pyl.unibe.ch

Abstract. We analyze extensively the temporal properties of the train of spikes emitted by a simple model neuron as a function of the statistics of the synaptic input. In particular we focus on the asynchronous case, in which the synaptic inputs are random and uncorrelated. We show that the NMDA component acts as a non-stationary input that varies on longer time scales than the inter-spike intervals. In the subthreshold regime, this can increase dramatically the coefficient of variability (bringing it beyond one). The analysis provides also simple guidelines for searching parameters that maximize irregularity.

1 Introduction

Spike trains recorded from single cells in vivo appear rather irregular. The origin of this high degree of variability has been debated in the last decade (see e.g. [3, 4]) and many authors suggested that input synchronization is necessary to achieve such a high variability (see e.g [2, 5]). While it is easy to show that input synchronization leads to high irregularity, it is difficult to rule out the possibility that the same variability can be achieved with asynchronous inputs. Proving this kind of negative results requires clear guidelines that allow to explore systematically the parameters space. Here we start by simulating the *in vitro* experiment described in [2] in which the authors were not able to obtain high variability with asynchronous inputs. We show that it is possible to achieve high irregularity without synchronicity and that synaptic NMDA receptor conductance may play an important role.

2 Methods

We simulate a single compartment leaky integrate-and-fire neuron whose dynamics is fully described by the membrane depolarization V:

$$\frac{dV}{dt} = -\frac{V(t) - V_{rest}}{\tau_m} + \frac{I_{syn}}{C_m}$$

where I_{syn} is the total synaptic current flowing into the cell, V_{rest} is the resting potential, τ_m is the membrane time constant and C_m is the membrane

capacitance. When $V(t)$ crosses a threshold V_θ, a spike is emitted and the depolarization is reset to V_{reset}, where it is forced to stay for a time interval τ_{arp} – the absolute refractory period. The parameters were chosen to reproduce the behavior of the real cells recorded in [2]: $\tau_m = 25ms, V_{rest} = -62mV, V_\theta = -27mV, V_{reset} = -42mV, \tau_{arp} = 5ms$. Since the model of the neuron is highly simplified, these parameters must be considered as 'effective' parameters. The arrival of a pre-synaptic spike induces a change in the conductance $g(t)$ which, in turns, injects a current $I(t)$ into the cell. For AMPA and fast GABA receptors we have: $I_{ampa,gaba}(t) = g_{ampa,gaba}(t)[V(t) - E_{rev}^{ampa,gaba}]$, where $E_{rev}^{ampa,gaba} = -10, -62mV$ are the reversal potentials. For NMDA receptors we have an extra factor that takes into account the voltage-dependent block of open NMDA receptors by extracellular magnesium (as in [2]). $g(t)$ is proportional to the fraction of open channels through a factor $\bar{g}$, and the time course of a unitary event is characterized by the raise time τ_r and the decay time τ_d that are respectively 5 and 150 ms for NMDA receptors, 0.5 and 2 for AMPA, and 0.5 and 7 ms for GABA. The total afferent current is constructed by summing linearly the unitary events coming from N_e excitatory and N_i inhibitory pre-synaptic neurons that fire at random times. The inter-spike intervals are distributed exponentially, as in a Poisson process, and each pre-synaptic excitatory spike activates both the AMPA and the NMDA conductances. All the parameters characterizing the synaptic input are identical to those in [2].

3 Results

Single receptor conductance. This case is useful to illustrate the properties of the NMDA component of the synaptic current. To simplify this preliminary analysis we momentarily drop the dependence of the input current on the membrane potential. There are known cases in which this simplification does not change much the statistics of the input current [1]. For independent inputs the input current is Gaussian and hence fully characterized by its mean $\mu = N\bar{g}\nu\tau_d$ and its variance $\sigma^2 \sim N\bar{g}^2\nu\tau_d$. We consider now the plane (μ, σ). Given N, ν and τ_d, the points lie on a line with slope $1/\sqrt{N\nu\tau_d}$. One can move along the line by changing g (see Fig. 1). In order to have elevated variability in the inter-spike intervals, the neurons should operate in a sub-threshold, fluctuations dominated regime, i.e. μ should stay below the threshold current μ_θ and σ should be large enough to drive the neuron across the threshold at a reasonable rate. The maximal ratio between the amplitude of the fluctuations and the average current is achieved when μ is just below μ_θ. To further increase this ratio one has to jump onto another line, i.e. to change one of the parameters that determine the slope. Smaller numbers N of afferents, shorter time constants τ and lower frequencies permit larger fluctuations.

NMDA conductance only. Complete simulations of the model confirm this picture (Fig. 2). As $\nu_e N_e$ is progressively reduced (diamonds: $\nu_e N_e = 800Hz$, triangles: $\nu_e N_e/2$, squares: $\nu_e N_e/4$, left part of the figure) the curves of the coefficient of variability (CV, ratio of standard deviation to the average of the

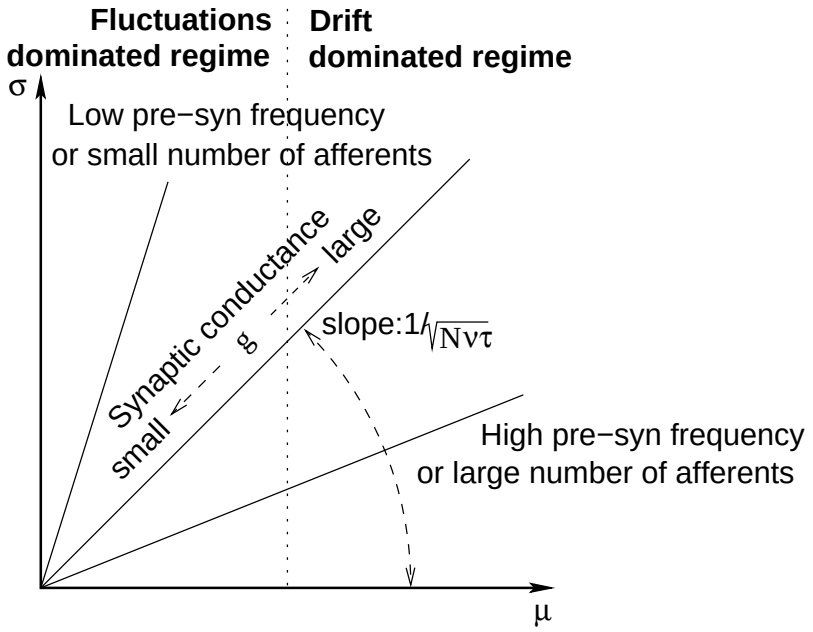

Fig. 1. The parameter space (μ, σ) characterizing the mean and variance of the synaptic current. Any pair (μ, σ) can be obtained by an appropriate choice of the average synaptic strength $\bar{g}$ and the product $N\nu\tau_d$, with N the number of afferents, ν their average frequency, and τ_d the decay time constant of the current. The fluctuation and drift dominated regimes are distinguished by a value of μ lower or higher than μ_θ (vertical dotted line), respectively. When changing $\bar{g}$ (as done in the following plots, Figs. 2-4) one moves radially along a straight line with slope $1/\sqrt{N\nu\tau_d}$.

inter-spike intervals) shift up, more prominently in the high rates region. Halving ν corresponds to jumping on a steeper line in Fig. 1 which allows to extend the fluctuations dominated regime to higher $\bar{g}_{nmda}$. Note that a reduction of $\nu_e N_e$ must be compensated by an increase of $\bar{g}_{nmda}$ to preserve the same output rate. Hence the intervals of variation for $\bar{g}_{nmda}$ are different for the three different curves. Note that this is equivalent to an increase of spatial correlation in the input. The dependence of the CV on τ_{nmda} is illustrated in the right part of the figure: diamonds, triangles and squares correspond respectively to $\tau_{nmda} = 150, 75, 37.5ms$. Smaller τ_{nmda} lead to steeper lines, which is reflected by an upwards shift of the CV in the supra-threshold region, as expected. In the sub-threshold regime instead, the temporal structure of the input current is dominant: long τ_{nmda} give rise to a slowly modulating component which increases the maximal CV [6, 7], although the ratio σ/μ is decreased (see also below). For $\tau_{nmda} \to 0$ these curves tend to the AMPA case for which the upper

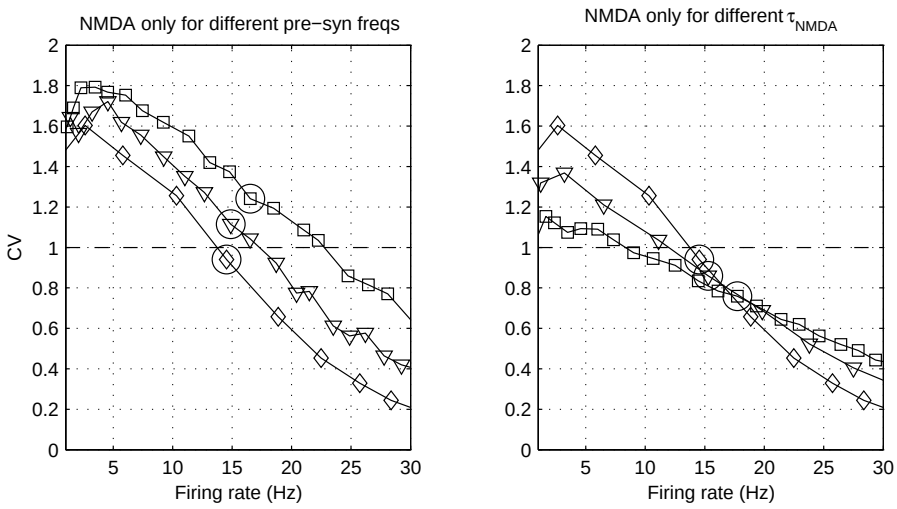

Fig. 2. Only NMDA component is present: coefficient of variability (CV) vs the neuron's own output rate for different pre-synaptic frequencies (left) and for different τ_{nmda} (right). Each point of a curve is obtained by moving $\bar{g}_{nmda}$ along the straight line at σ/μ constant (see Fig. 1) in order to have the desired output frequency (between 1 and 30 Hz). For different curves, different $\bar{g}_{nmda}$ ranges are swept in order to have the same range of output rates. This procedure allows to compare CVs at parity of firing rate. Those points that are circled correspond to the threshold current μ_θ that separates the fluctuations dominated regime (sub-threshold) and the drift dominated regime (supra-threshold). In the left panel $N\nu = 800$ Hz (diamonds), 400 Hz (triangles) and 200 Hz (squares). In the right panel $\tau_{nmda} = 150$, 75 and 37.5 ms (same symbol code). The ranges of $\bar{g}_{nmda}/C_m$ (nS) are (left panel) $(2.6, 3.5)$ (diamonds), $(5, 7)$ (triangles) and $(9.5, 14)$ (squares); (right panel) $(2.6, 3.45)$, $(5.2, 7.2)$, and $(10.8, 15.7)$.

bound is $CV = 1$.

NMDA and AMPA conductances. The relative contribution of the AMPA component to the fluctuations grows quadratically with g and hence it usually dominates over the NMDA part. The AMPA component permits higher σ/μ ratios and extends to higher frequencies the fluctuations dominated regime. However the relatively short time correlation length limits the maximal CV to 1. The NMDA component acts as a temporal modulation of the average current on time scales that are longer than the inter spike intervals. This modulation increases the upper bound of the CV (see Fig. 3).

The role of inhibition. Increasing g leads to larger fluctuations, but, at the same time, to larger average currents, bringing the cell close to a drift dominated regime. However, in the presence of inhibition, the average current and the fluctuations can become independent and the amount of noise increase without moving the average too close to the threshold. In the presence of inhibition it is therefore much simpler to achieve large CVs on a wide range of frequencies.

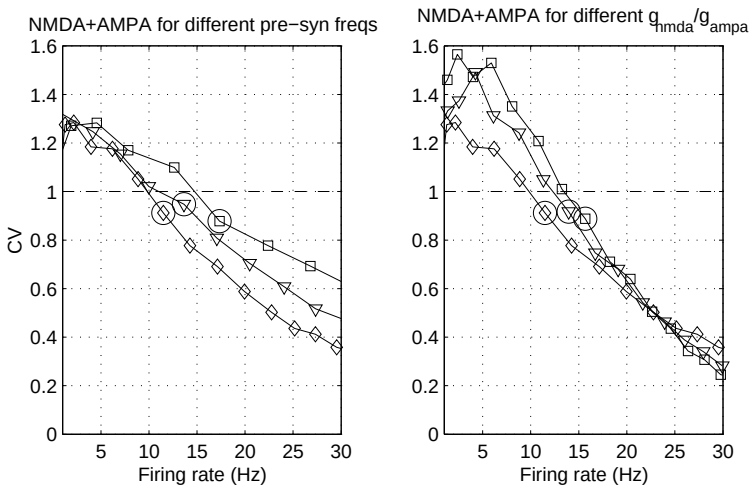

Fig. 3. NMDA and AMPA components. CV vs output rate for different pre-synaptic frequencies (left) and for different ratios $\bar{g}_{ampa}/\bar{g}_{nmda}$ (right). The curves are generated as in Fig. 2. The arrow indicates the experimental point of [2]. Left: The pre-synaptic frequencies are: diamonds: $\nu_e N_e = 800Hz$, triangles: $\nu_e N_e/2$, squares: $\nu_e N_e/4$. The ratio $g_{ampa}/g_{nmda} = 10$. CVs are smaller than in Fig. 2 but the curves are qualitatively the same. The differences between the three curves are more evident in the supra-threshold regime, where higher σ/μ ratios due to low pre-synaptic frequencies allow for a wider range of high CVs. Since the relative strength of AMPA and NMDA components is kept fixed, so is the correlation length and the maximal CV (achieved in the sub-threshold regime) is not affected much by a change in the pre-synaptic frequencies. Right: the three curves correspond to different ratios $r = \bar{g}_{ampa}/\bar{g}_{nmda}$: diamonds: $r = 10$, triangles: $r = 5$, squares: $r = 2.5$. As the NMDA component increases, the maximal CV also increases. The supra-threshold regime is not affected by r: the NMDA component does not change the variability at high rates where the temporal aspects of the input current are less important than the relative strength of the fluctuations. The ranges of $\bar{g}_{nmda}/C_m$ (nS) are (left panel) $(1.7, 2.3)$ (diamonds), $(3.2, 4.7)$ (triangles) and $(5.8, 9.4)$ (squares); (right panel) $(1.7, 2.3)$, $(2.1, 2.7)$, and $(2.3, 3.1)$.

In Fig. 4 we show one example in which $\bar{g}_{gaba}$ increases linearly with $\bar{g}_{nmda}$ and $\bar{g}_{ampa}$. The CV remains almost constant throughout the full range 1-30 Hz.

4 Conclusions

We showed that high variability in the inter-spike intervals can be achieved without any synchronization of the inputs provided that the parameters are chosen appropriately. The intervals that allow high CV depend on the number of afferents, the mean pre-synaptic frequencies and the time correlation length of the receptors. The high CV range can be quite reduced if inhibition is not included. However, even without inhibition, high CVs can be achieved in biologically plausible ranges. Two factors turn out to be important: 1) the possibility of keeping

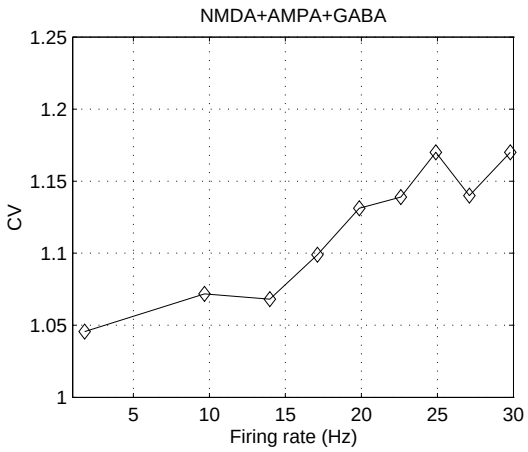

Fig. 4. CV vs output rate in the presence of inhibition. $\nu_e N_e = 800Hz$, $\nu_i N_i = 600Hz$ as in [2]. $\bar{g}_{nmda}/Cm$ range: $(0.09, 9)$ nS, with $\bar{g}_{ampa} = 10\bar{g}_{nmda}$, $\bar{g}_{gaba} = 4.7\bar{g}_{nmda}$ throughout.

the neuron in the fluctuations dominated regime (see e.g. [3]); 2) a (long enough) time correlation length, as that of NMDA receptors. For large fluctuations, in a sub-threshold regime, the CV can always reach 1, although the corresponding frequencies might be too low to be measurable. The NMDA component is equivalent to a non-stationary input current that varies on longer time scales than inter-spike intervals. This non-stationarity can bring the CV above 1 [6, 7], surpassing the upper bound for uncorrelated processes.

References

1. Amit D.J. and Tsodyks M.V., Effective neurons and attractor neural networks in cortical environment, *NETWORK* **3**:121-137 (1992)
2. Harsch A. and Robinson H.P.C., Postsynaptic variability of firing in rat cortical neurons: the roles of input synchronization and synaptic NMDA receptor conductance, *J. Neurosci.* **16**:6181–6192 (2000)
3. Shadlen M.N. and Newsome W.T., The variable discharge of cortical neurons: implications for connectivity, computation and information coding, *J. Neurosci.* **18**(10):3870-3896 (1998)
4. Softky W.R. and Koch C., The highly irregular firing of cortical cells is inconsistent with temporal integration of random EPSPs, *J. Neurosci.* **13**(1):334 (1993)
5. Stevens C.F. and Zador A.M., Input synchrony and the irregular firing of cortical neurons, *Nature Neuroscience* **1**:210-217 (1998)
6. Svirskis G. and Rinzel J., Influence of temporal correlation of synaptic input on the rate and variability of firing in neurons, *Biophys. J.* **5**:629-637 (2000)
7. Troyer T.W. and Miller K.D., Physiological gain leads to high ISI variability in a simple model of a cortical regular spiking cell, *Neural Comput.* **9**:971-983 (1997)

This article was processed using the LaTeX macro package with LLNCS style